REPORT DOCUMENTATION PAGE

Form Approved OMB No. 0704-0188

1. REPORT DATE *(DD-MM-YYYY)*	2. REPORT TYPE	3. DATES COVERED *(From – To)*
26-10-2009	Final Report	26 September 2008 - 02-Feb-10

4. TITLE AND SUBTITLE

Development of a PLIF Imaging Diagnostic for Turbulent Combustion Applications with Sustained kHz Repetition Rate

5a. CONTRACT NUMBER
FA8655-08-1-3058

5b. GRANT NUMBER

5c. PROGRAM ELEMENT NUMBER

6. AUTHOR(S)

Dr. Isaac G Boxx

5d. PROJECT NUMBER

5d. TASK NUMBER

5e. WORK UNIT NUMBER

7. PERFORMING ORGANIZATION NAME(S) AND ADDRESS(ES)

Deutsches Zentrum fur Luft- und Raumfahrt
Pfaffenwaldring 38-40
Stuttgart 70569
Germany

8. PERFORMING ORGANIZATION REPORT NUMBER

N/A

9. SPONSORING/MONITORING AGENCY NAME(S) AND ADDRESS(ES)

EOARD
Unit 4515 BOX 14
APO AE 09421

10. SPONSOR/MONITOR'S ACRONYM(S)

11. SPONSOR/MONITOR'S REPORT NUMBER(S)
Grant 08-3058

12. DISTRIBUTION/AVAILABILITY STATEMENT

Approved for public release; distribution is unlimited.

13. SUPPLEMENTARY NOTES

14. ABSTRACT

This report results from a contract tasking Deutsches Zentrum fur Luft- und Raumfahrt as follows:
Consistent with the reporting requirements listed in Section VI.2 of AFOSR BAA 2007-1, progress towards meeting the goals specified in this proposal will be reported in an annual technical brief and a final technical and financial report upon completion of the project. Copies of publications resulting from this work shall be included with the final technical report.

15. SUBJECT TERMS
EOARD, Turbulent Combustion

16. SECURITY CLASSIFICATION OF:			17. LIMITATION OF ABSTRACT	18, NUMBER OF PAGES	19a. NAME OF RESPONSIBLE PERSON
a. REPORT	b. ABSTRACT	c. THIS PAGE			SURYA SURAMPUDI
UNCLAS	UNCLAS	UNCLAS	UL	15	19b. TELEPHONE NUMBER *(Include area code)* +44 (0)1895 616021

Final Report

Development of a PLIF Imaging Diagnostic for Turbulent Combustion Applications with Sustained kHz Repetition Rate

Dr. Isaac Boxx

Background

The objective of this project was to complete the assembly, validation and optimization of a multi-kHz frame-rate planar Laser-induced fluorescence imaging system that was being developed at the German Aerospace Center - Institute for Combustion Technology and to demonstrate its capabilities by applying it to the study of a well-characterized, turbulent non-premixed jet-flame. The duration of the proposed project was 12 months and work was to be completed in two phases. The first phase of this project involved the assembly, alignment, testing and optimization the various individual components of the system. During this period timing, control and data-analysis software for the system were also to be written. The second phase of the project was to be devoted to the acquisition and analysis of a series of high-framerate (1 – 5kHz), time-resolved planar-LIF measurements of the flowfield of a standard well-characterized, non-premixed, jet-flame. Each of these objectives has been met and significantly surpassed.

High Framerate Planar Measurement System

The kHz-PLIF measuring system consists of two independent PLIF systems, which may be operated simultaneously or separately. The first of these systems is optimized around a 5 kHz repetition rate. The second is designed for operation around 10 kHz. Both have similar spatial resolution and signal to noise ratios (SNR). Although separate from the

EOARD project described in this report, a high framerate PIV system was simultaneously developed at the DLR Institute for Combustion Technology and comprises part of the system. As this system was applied in the same set of measurements on the DLR-B (Bergmann et al., 1998) turbulent non-premixed jet-flame, it is also described below.

5 kHz Laser

The 5 kHz PLIF system used a frequency-doubled dye laser (Sirah Cobra-Stretch HRR), pumped with a frequency-doubled, diode-pumped solid state Nd:YLF laser (Edgewave IS-8IIE), operating at 523 nm. At 5 kHz, the pump laser delivered 3.8 mJ/pulse (19 W average output) with 8.5 ns pulse duration. Due to the relatively low pulse energy of the pump-laser, the dye laser uses only an oscillator and pre-amplifier (in a single dye cell) and has no main amplifier. To avoid bleaching of the dye, (Rhodamine 6G in Ethanol, 0.09g/L concentration), at these high repetition rates, the laser was equipped with a high flowrate dye pump; in addition, the dye solution was cooled using a heat-exchanger within the dye reservoir. A BBO crystal was used for frequency doubling of the dye beam. Conversion efficiency in this crystal ranged from 10 to 17%, depending on repetition rate (and hence the fluence of the incoming beam). The BBO crystal was passively heated by the laser and thus had to be run for sufficient time prior to each measurement to allow it to thermally stabilize. Isolation of the fundamental and frequency-doubled beams was accomplished with a four-prism separator. At a 5 kHz pump frequency, the time-average output from the dye laser at 282.6 nm was ≈ 0.5 W or 100 μJ/pulse.

10 kHz Laser

The 10 kHz PLIF system uses a frequency-doubled dye laser (Sirah Credo), pumped with a frequency-doubled, diode-pumped solid state Nd:YAG laser (Edgewave IS-8IIE), which operated at 532 nm wavelength. At 10 kHz, the pump laser delivered 4 mJ/pulse (40 W

average output) with 8.5 ns pulse duration. This dye laser uses a low-threshhold resonator cavity optimized for the relatively low pulse energies associated with kHz-rate pump lasers. As a result, this laser is considerably more efficient than the 5 kHz laser, and thus uses separate resonator and amplifier dye cell. As with the 5 kHz system, the laser was equipped with high flowrate dye pumps, which were actively cooled using heat-exchangers within each dye reservoir. A BBO crystal was used for frequency doubling of the dye beam. The BBO crystal in this laser is equipped with an active temperature control oven to maintain peak efficiency and thermal stability over a wide operating range. Isolation of the fundamental and frequency-doubled beams was accomplished with a four-prism separator. At 10 kHz pump frequency, the time-average output from the dye laser at 282.6 nm was ~1.4 W or 140 μJ/pulse. Although higher pulse energies are possible with the same pump laser, this comes with an increased risk of damaging either the BBO frequency-doubling crystal or the four-prism wavelength separation unit. As such, the laser was operated at 1 – 1.4 W during the experiments for this study.

Sheet Forming Optics

The 283 nm beams were formed into sheets of ≈ 40 mm (high in the probe region) using fused silica lenses (f_{plif1} = -25 mm, f_{plif2} = 250 mm) in a cylindrical telescope configuration and focused to a waist using a third cylindrical lens (f_{plif3} = 500 mm). All optics were anti-reflective coated to minimize pulse energy losses before the measurement region. In experiments where PIV was accomplished simultaneously with the OH-PLIF, the 283 nm laser sheet was overlapped with the PIV laser sheet by transmitting the (532 nm wavelength) PIV sheets through a 283-nm turning mirror (see Fig. 1). The PIV and PLIF sheets were overlapped in the near and far fields and also in the probe region. Sheet thicknesses were measured by translating a narrow slit through each beam and using a photodiode to record the

spatial distribution; with this approach the 283 nm beam was determined to be ~400 μm at the probe volume.

The wavelength tuning of the dye lasers to the peak of the isolated $Q_1(6)$ line of the A-X (1-0) transition of OH was checked daily using a setup consisting of a laminar reference flame, a 10 cm monochrometer (Jobin Yvon H10-UV) and a photomultiplier tube for fluorescence detection. The laser line width at 566 nm was 0.06 cm^{-1} for each system.

Intensified Imaging System

The resulting fluorescence was acquired with high frame-rate CMOS cameras (LaVision HSS5) and external, two-stage, lens-coupled intensifiers (LaVision HS-IRO). The intensifiers use 25mm diameter S20 photocathodes and P47 phosphor in their first stage, and S20T / P46 for the second (booster) stage. The HSS5 cameras each have an array of 1024 × 1024 pixels, which are 17-μm square and digitized to 10-bit. The cameras operate in full-frame mode at 3000 frames per second (fps) and contain on-board memories of 2.6 GB. This corresponds to approximately 0.8 second of acquisition time at maximum frame rate and resolution for each camera.

Fluorescence signal was collected at 310nm with a fast Cerco 45mm, f/1.8 or Halle 100 mm, f/2 lens, depending on the desired field of view and stand-off distance. The lenses were mounted to the external intensifiers, and both intensifiers and cameras were mounted on rails to more easily adjust the field of view. Background luminosity was reduced using a 500-ns intensifier gate. Elastic scattering at 283 nm was blocked using a high-transmission (> 80% at 310 nm) bandpass interference filter (Custom fabrication - Laser-Components GmbH). Flat-field correction for spatial variation of the laser sheet-intensity and other imaging nonuniformities was accomplished using a mean image derived from laser-induced fluorescence of acetone that was doped into the co-flow of the jet-flame burner (to be

described later). Run-to-run background and camera noise was corrected using a 1000 frame ensemble average acquired while the lasers were blocked.

Particle Image Velocimetry System

The PIV system is based on a dual-cavity, diode-pumped, solid state Nd:YAG laser (Edgewave, IS-611DE) and a CMOS camera (LaVision HSS6). The laser produces 2.6 mJ/pulse at 532 nm at repetition rates of up to 10 kHz. Pulse duration is ≈ 14 *ns*. Pulse timing separation for the PIV system in this study was set to Δt = 10 μs, with the OH-PLIF excitation pulses temporally interlaced between the first and second PIV pulse of a measurement cycle. As with the PLIF system, three cylindrical lenses were used to form the sheet: f_{piv1}= -25 mm, f_{piv2} = 300mm, and f_{piv3} = 1000 mm. To minimize noise arising from inter-frame particle dropout, the beam waist was located somewhat beyond the probe region. The sheet thicknesses were measured in the same manner as for the PLIF beam; at the probe volume, the sheet thicknesses were ≤ 0.7 mm. Mie scattering from titanium dioxide (TiO_2) particles seeded into the flow was imaged using a CMOS camera mounted nearly perpendicular to the laser sheet. The camera has a 12-bit, 1024 × 1024 pixel imaging array (20 μm square pixels) and is capable of imaging at up to 5400 fps in full frame mode. Operated in two-frame PIV mode at 10 kHz, this array size is reduced to 512 × 512 pixels. The PIV camera has sufficient on-board memory (8 GB) to match the acquisition time of the OH-PLIF cameras in a given experiment run. Scattered light was collected with a Nikon, AF-Nikkor 200-mm focal length lens and image-blur due to off-axis defocusing was corrected using a Scheimpflug adaptor between the lens and camera. The relatively short integration time (50 μs) eliminated the need for interference or coloured-glass filters in front of the lens. Perspective distortion was corrected using an imaging target composed of an array of equidistant spaced round dots. The same target was used to map the fields of view of the PIV and PLIF systems to one another. Image mapping, calibration, and particle cross-correlations

were completed using a commercial, multi-pass adaptive window offset cross-correlation algorithm (LaVision DaVis 7.2). Final window size and overlap were 16 × 16 pixels and 50%, respectively. The field-of-view imaged by the PIV system was 12 mm x 11 mm, resulting in a spatial resolution and vector spacing of approximately 0.34 mm and 0.17 mm respectively.

DLR-B Target Flame

The flame studied in this project was a round, turbulent, non-premixed jet flame known as the 'DLR-B' flame. The DLR-B has served as a target flame for the Turbulent Non-Premixed Flame (TNF) workshop and has been extensively studied and characterized with a wide variety of experimental and numerical techniques (Bergmann et al., 1998). The DLR-B flame consists of a fuel jet issuing from an 8 mm inner-diameter tube into a concentric co-flow of low-velocity air. The fuel jet is a mixture containing 22.1% CH_4, 33.2% H_2, and 44.7% N2 by volume and has a mean exit velocity of 63.2 m/s. This corresponds to a jet-exit Reynolds number of $Re_d = 22\,800$, based on room temperature fluid properties. The mean co-flow velocity was ≈ 0.3 m/s. The DLR-B flame operates close to the blow-off limit for this fuel mixture and exhibits frequent local extinction and re-ignition events. Such events are of both fundamental and technical interest to the combustion community and were therefore the primary focus of this experiment.

It should be noted that the target flame in this study differs in one regard from some earlier studies on the DLR-B flame, in that both the main flow and the low-velocity co-flow were seeded with TiO_2 particles of approximately 1 μm diameter. This particle seeding was necessary to allow for time-resolved, 2-D PIV measurements however, if such seeding is used excessively, it has the potential to affect the local extinction and re-ignition characteristics. Thus, a rigorous check of the flame-holes statistics for the seeded jet flame against those of an unseeded DLR-B flame was made. This check showed no difference in the flame-hole size or frequency between the two and we therefore conclude the particle seeding does not

measurably affect the local-extinction or re-ignition phenomena. The data set from this experiment can therefore be directly compared to previous studies of the DLR-B flame.

Measurement Campaign

The experiment configuration is shown in Fig. 1. Various elements of the complete planar measurement system have been tested and demonstrated in a variety of turbulent flames of both fundamental and applied interest (Boxx et al., 2009a, b and c). A key goal of the present work was to demonstrate the complete working system and realize its full potential by utilizing all three imaging systems simultaneously in the study of a turbulent flame. Thus, measurements focusing on local flame-extinction and re-ignition events in the DLR-B target flame were performed at the DLR Institute for Combustion Technology in Stuttgart over the period of April through May, 2009. These measurements were performed in collaboration with Dr. Jonathan Frank, of the Combustion Research Facility of Sandia National Laboratories. DLR Co-workers Dr. Wolfgang Meier, Dr. Adam Steinberg and Mr. Christof Arndt also participated in the measurement campaign and subsequent data analysis. This campaign resulted in the acquisition of approximately 330 GB of scientific and technical data.

In these measurements, the DLR-B target flame was imaged simultaneously in two planes using OH PLIF, while two-component PIV measurements were acquired simultaneously in one of the planes. PIV and PLIF measurements were acquired at 10 kHz in the plane aligned to the central axis of the jet, while OH PLIF was acquired at 5 kHz (i.e. on every second measurement cycle) in a plane inclined 40° to the horizontal. The decision to image an oblique plane was driven by the need to identify and condition flame-extinction events with knowledge of out-of-plane flame sheet behavior. This is not possible when imaging only a single plane. Ideally, the second plane would be perpendicular to the first however restrictions on optical access prevented this.

The simultaneous PIV / PLIF measurements were acquired at an axial location of 10 diameters downstream of the jet-exit. An excellent set of 2-D planar measurements of the flame at this location, acquired at low repetition rates (several 10's of Hz), are available for direct comparison in Kaiser and Frank (2009). These indicate such events are highly transient and influenced by local flow conditions and specific strain histories. This makes the current two-plane, time-resolved flame-front / velocity field measurements both an excellent demonstration of the capabilities of the kHz planar measurement system, and an exceptionally useful tool for studying such phenomena.

Results and Discussion

Given the large quantity of high quality measurements acquired in this study, data reduction and analysis is not yet complete. To date, the PIV images have been processed to extract usable velocity vectors and all appropriate image mapping, sheet-, camera-sensitivity and background-correction routines have been applied to the PLIF measurements. With the raw data now in a usable form, efforts are currently focused on developing automated data-reduction, pattern recognition, flow-feature tracking and statistical tools directly applicable to the kind of time-resolved flame front / velocity field data acquired in this project. An overview of the processing techniques we are developing is presented below.

Figure 2 shows a pair of sample OH-PLIF images acquired in this study. The first frame shows the OH distribution in the oblique plane at a downstream location of 80 mm (x/D=10). At this location the OH distribution represents quite well the reaction zones and may be understood as a planar cut through the flame sheet. The flame is close to blowout and several positions where local flame extinction interrupts the flame front can be seen. The dashed line shows the plane where the second, vertical OH PLIF and the PIV sheets were located. The second frame of Fig. 2 illustrates the OH distribution in this plane and enables an estimation of the size of the flame hole in the axial direction. With the long image sequences

from the measurements it was possible to analyze the temporal development of the flame holes from their appearance to the growth to maximum size and the final shrinking and mending. In addition, the corresponding PIV sequence enabled the determination of the influence of the flowfield on this development.

Identification and tracking of flame-holes

A key advantage of long-duration time-resolved, planar measurements is that they provide the new capability to identify and track the progression of temporally unpredictable phenomena through a flow field. This enables conditioning of flowfield statistics on specific classes of flow field / flame interactions, such as local extinction and re-ignition. The focus of our analysis is just such a statistical conditioning of flowfield phenomena.

In this work, flame-holes were identified in a manner similar to Kaiser and Frank (2009), who showed that holes appear as gaps in an otherwise continuous OH layer. Initially, only flame holes appearing in the vertical measurement plane are considered, as these are most relevant for comparison to existing studies. Following the procedure of Kaiser and Frank (2009), the OH images were filtered with a 0.5 mm square filter and converted to binary using a global intensity threshold. Flame-holes were then identified based the shortest straight-line distance between adjacent regions of OH. Incorrectly identified flame holes (i.e. those between non-adjacent OH regions) were removed by selecting the flame-hole combination that connected the islands with the minimum total path length. Mathematically, each flame-hole may then be treated as a vector,

$$\tilde{h}_i(t) = \tilde{x}_{i1}(t) + l_i(t)\tilde{\xi}_i(t) \qquad (1)$$

where $\tilde{x}_{i1}(t)$ represents a particular end of the flame-hole, $l_i(t)$ is the length of the flame-hole, and $\tilde{\xi}_i(t)$ is a unit vector pointing along the flame-hole from $\tilde{x}_{i1}(t)$ to its opposite end, $\tilde{x}_{i2}(t)$. For consistency, $\tilde{x}_{i1}(t)$ was defined as the end of the flame-hole with the lowest axial position.

The flame-holes thus identified were tracked through measurement sequences in a Lagrangian manner (i.e. by following the fluid) using the simultaneously acquired PIV velocity data. Two important tracking abilities are required for this analysis. First, it is necessary to identify the same flame-hole in subsequent images. To do so, a square control volume $\overline{V}_{i1}(t)$ was defined around each detected flame-hole. The rows of $\overline{V}_{i1}(t)$ represent the (x, y) coordinates of the velocity measurement locations within the volume. The mean velocity within $\overline{V}_{i1}(t)$ was then computed and used to provide a first estimate the displacement of the control volume between frames:

$$\overline{V}_{i1}(t_0 + \Delta t) = \overline{V}_{i1}(t_0) + u(\overline{V}_{i1}(t_0), t_0)\Delta t \tag{2}$$

where $\overline{V}_{i1}(t_0 + \Delta t)$ represents the estimate for the control volume location at the next measurement time and $u(\overline{V}_{i1}(t_0), t_0)$ is the mean velocity in $\overline{V}_{i1}(t_0)$. However, the velocity field within the control volume may change between frames as the turbulence evolves. This would result in slightly incorrect displacements based on Eq. 2 that could lead to smaller holes being incorrectly tracked. Therefore, an iterative procedure was implemented, where the convective velocity of the control volume was taken to be the mean of the velocity field within $\overline{V}_{i1}(t_0)$ and $\overline{V}_{i1}(t_0 + \Delta t)$. This was repeated until the displacement of $\overline{V}_{i1}(t_0 + \Delta t)$ changed by less than 5% between iterations.

The corresponding flame-hole at the next time step, $\tilde{h}_i(t + \Delta t)$, was then selected to be the flame-hole within the final $\overline{V}_{i1}(t_0 + \Delta t)$. If multiple flame-holes are present in $\overline{V}_{i1}(t_0 + \Delta t)$, the hole that most closely matches the orientation of $\tilde{h}_i(t_0)$ is selected. Various additional conditions and checks are currently being implemented to improve the robustness of the tracking routine. These include a recursive process that selects the best total path for two adjacent flame-holes convecting together and a check to prevent new flame-holes (either

newly generated or those convecting into the measurement plane) from incorrectly being identified as the continuation of a flamehole from a previous frame.

A comparison of the flame-holes tracked by the algorithm and those identified manually indicated that the algorithm correctly selected the flame-hole approximately 90% of the time. Flame-hole identification errors typically occurred in situations where a new flame-hole appeared in the measurement plane closely adjacent to a existing hole. However, such time sequences were rare and often involved out-of-plane convection of holes through the vertical measurement plane. Such sequences were not tractable for the subsequent analysis of flame-hole reignition and were therefore excluded from consideration.

The second important parameter that must be tracked through time is the location of the flame edges. This is important in order to compute the local displacement speed of the flame S_D, defined as the velocity of the flame sheet relative to that of the local fluid velocity. The location to which each hole endpoint, $\tilde{x}_{ij}(t)$, would passively convect was determined using the same iterative procedure that was used for the control volumes. An average of the four velocity measurements in a square around the exact hole endpoints was used to determine the convective velocity. The difference between the absolute measured flame edge location and the computed passive convection distance is best explained by flame propagation via chemical reaction.

It must be noted that the exact flame-hole geometry is somewhat dependent on the particular OH signal threshold applied. Two threshold levels therefore were tested for this study, with the second being 25% higher than the first. It was found that the statistical results were independent of the threshold level over this range and that the results from individual extinction events were qualitatively and phenomenologically independent of the threshold chosen. Hence, results from only the lower threshold will be considered in our ongoing analysis.

Reduction of out-of-plane convection effects

Another important point to consider in the Lagrangian tracking routines is that out-of-plane convection of the flame-holes would erroneously appear as re-ignition due to edge flame propagation in the vertical measurement plane. Hence, once flame-holes had been identified and tracked in the vertical imaging plane, the (simultaneously acquired) OH-PLIF images from the oblique measurement plane were used to identify and remove unsuitable holes from the subsequent re-ignition analysis. This was accomplished by taking flame-holes identified in the vertical measurement plane and matching them to the corresponding holes in the oblique measurement plane, based on their temporal and spatial locations. The center of each matched hole in the radial direction was then determined. Using a simple geometric model we are able to estimate the amount of through-plane convection for a given hole and determine the apparent rate of flame propagation caused by this convection. For example, a constant size flame hole with diameter 2 mm that convects less than 10% of its own diameter out-of-plane between measurements would exhibit an apparent re-ignition rate in the vertical plane of approximately 0.06 m/s. In the present study, only events for which the apparent re-ignition rate due to out of-plane convection is less than a certain threshold will be included in the subsequent analysis. This threshold will be determined based on being able to accurately limit through-plane convection uncertainty to a percentage of the most probable flame propagation speed.

Summary

A combined planar laser-induced fluorescence (PLIF) and particle image velocimetry (PIV) system capable of quasi-continuous operation at multi-kHz framerates was developed and successfully demonstrated. The total system consists of two independent multi-kHz framerate PLIF systems; one optimized around 5 kHz and the other around 10 kHz, and a 10 kHz PIV system. Each system is equipped with sufficient on-board memory for 0.8 – 1 s of

continuous image acquisition. The system was demonstrated in a series of measurements focussing on the dynamics of local flame-front extinction and re-ignition in the DLR-B turbulent, non-premixed jet flame. This measurement campaign yielded over 300 GB of scientific and technical data. A rigorous statistical analysis based on newly developed Lagrangian flame-hole tracking routines and conditional averaging of flow field properties is currently underway. Initial results of this analysis are being readied for submission in the form a paper for the 33rd International Combustion Symposium (2010), and a longer, more complete journal article to follow shortly thereafter.

References

V. Bergmann, W. Meier, D. Wolff, W. Stricker. "Application of Spontaneous Raman and Rayleigh Scattering and 2D LIF for the Characterization of a Turbulent $CH_4/H_2/N_2$ Jet Diffusion Flame", Appl. Phys. B 66, 489 (1998)

I. Boxx, M. Stöhr, R. Blumenthal, C. Carter, W. Meier, AIAA 2009-644, 47th AIAA Aerospace Sciences Meeting, 5-8 January (2009a).

I. Boxx, C. Heeger, R. Gordon, B. Böhm, A. Dreizler, W. Meier, Combust. Flame, 156 (2009b) 269-271.

I. Boxx, M. Stöhr, C. Carter, W. Meier, Appl. Phys B, 95:1 (2009c). 23-29.

S. A. Kaiser, J. H. Frank, Proc. Combust. Inst 32 (2009) 1639–1646.

Figures

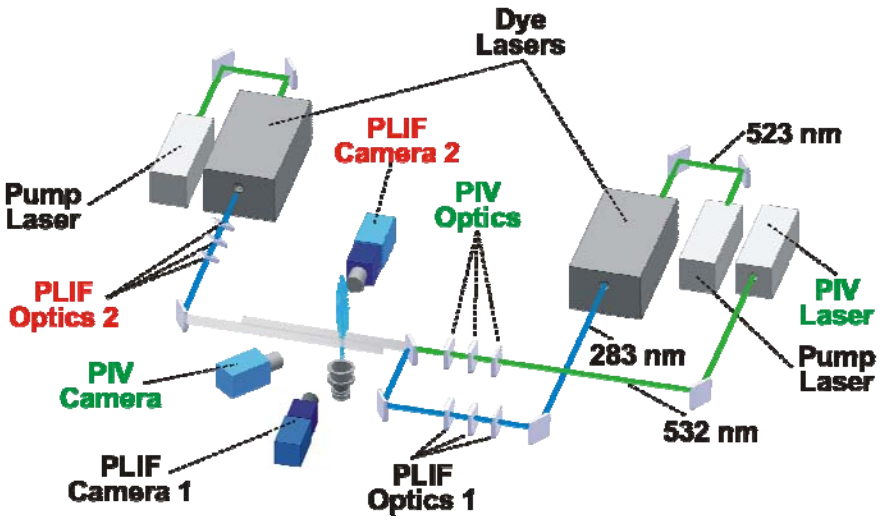

Figure 1. Experiment configuration

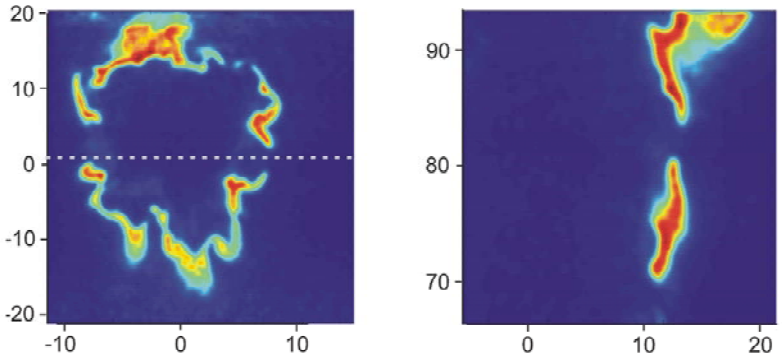

Figure 2. „Quasi-horizontal" and vertical OH LIF distributions simultaneously measured in a turbulent diffusion flame. The dashed line indicates the position of the vertical sheet. Numbers at the scales give radial and axial positions in mm.